

FAULT TOLERANT CONTROL FOR WIND TURBINE PITCH ACTUATORS

José Rodellar*, Leonardo Acho*, Christian Tutivén*, Yolanda Vidal*

*Universitat Politècnica de Catalunya, Applied Mathematics III, Escola Universitària d'Enginyeria Tècnica Industrial de Barcelona, Control Dynamics and Applications Research Group (CoDAIab)
Comte d'Urgell, 187, Barcelona, Spain

{jose.rodellar,leonardo.acho,christian.tutiven,yolanda.vidal}@upc.edu

Keywords: fault detection, fault identification, fault tolerant control, condition monitoring, wind turbine, pitch actuator, discrete-time, FAST.

Summary: *This paper develops a fault detection and isolation (FDI) and active fault tolerant control (FTC) of pitch actuators in wind turbines (WTs). This is accomplished combining a disturbance compensator with a controller, both of which are formulated in the discrete-time domain. The disturbance compensator has a dual purpose: to reconstruct the actuator fault (which is used by the FDI technique) and to design the discrete-time controller to obtain an active FTC. That is, the actuator faults are reconstructed and then the control inputs are modified with the reconstructed fault signal to achieve a FTC in the presence of actuator faults with a comparable behavior to the fault-free case. The proposed techniques are validated using the aeroelastic wind turbine simulator FAST. This software is designed by the U.S. National Renewable Energy Laboratory and is widely used for studying wind turbine control systems.*

1. INTRODUCTION

Fault detection and isolation (FDI) techniques (also called fault diagnosis) can be classified into two categories: signal processing based and model-based [1]. In the latter case, which is the approach used in this work, it is typical that a fault is said to be detected based on a residual signal. It must be a signal that is close to zero in the absence of a fault, and significantly affected in the presence of faults [2]. The main components of a fault detection system are the following: residual generator signal, residual evaluation method, and prescribed threshold to decide whether a fault occurs or not [2]. It is then the task of fault isolation to categorize the type of fault and its location. Recently, there has been a lot of interest in FDI in wind turbines (WTs). For example, observer based schemes are provided in [3], support vector machine based schemes are used in [4], data driven methods are used in [5], and [6] is based on a generalized likelihood ratio method.

In control systems for wind turbines, robustness and fault-tolerance capabilities are important properties which should be considered in the design process, calling for a generic and powerful tool to manage parameter-variations and model uncertainties. In this paper, an *active*

fault tolerant control (FTC) is provided capable to handle the parameter variations along the nominal operating point and robust to the faults in the pitch system. In *passive* FTC systems, controllers are predetermined and are designed to be robust against a class of presumed faults. This approach needs neither FDI schemes nor controller reconfiguration, but it has limited fault-tolerant capabilities. In contrast, *active* FTC reacts to the system component failures actively by reconfiguring control actions so that the stability and acceptable performance of the entire system can be maintained [7]. A successful *active* FTC design relies heavily on real-time FDI schemes to provide the most up-to-date information about the true status of the system [7]. The main goal in this work is to design a controller with a suitable structure to achieve stability and satisfactory performance, not only when all control components are functioning normally but also in case of (tolerable) faults. While still being a relatively new research topic, recent years have seen a growing number of publications in wind turbine FTC. For example, a set value based observer method is proposed in [8], and [9] proposes a control allocation method for FTC of the pitch actuators. A virtual sensor/actuator scheme is applied in [10]. Reference [11] presents an active FTC scheme based on adaptive methods and a model predictive control scheme is used for FTC in [12].

In terms of control, the wind turbine works in two distinct regions. One is below the rated wind speed, in the partial load region, where the turbine is controlled to maximize the power capture. This is achieved by adjusting the generator torque to obtain an optimum ratio between the tip speed of the blades and the wind speed. The other one is above the rated wind speed, in the full load region, where the main task of the controller is to adapt the aerodynamic efficiency of the rotor by pitching the blades into or out of the wind to keep the rotor speed at its rated value. Blade control pitching is activated only in the full load region, while in the partial load region the blades are kept by the controller at zero pitch angle [13]. In this paper, operation in the full load region, where the blade pitch control is acting, is considered.

Nowadays, pitch actuators are basically divided into two types: electric and hydraulic. Hydraulic actuators change the blade pitch angle through a hydraulic system. The method offers rapid response frequency, large torque, convenient centralization and is widely applied in WTs [14]. However, hydraulic systems may suffer from oil leakage, high air content in the oil, pump wear and pressure drop [15]. These faults are studied in this paper. In fact, the pitch actuators have the highest failure rate in WTs [15]. Thus, WT pitch sensors and actuators are often the topic of the FDI and FTC research focus. For example, an H-infinity- based FDI technique to detect and estimate the magnitude of blade bending moment sensor and pitch actuator faults is given in [16]; blade root bending measurements are used to detect pitch misalignment in [17]; model-based and system identification techniques are used for pitch actuator faults in [18].

The main contribution of this paper is twofold. First, a controller based on a disturbance compensator is proposed to face with tolerable faults. Second, a fault-diagnosis algorithm is developed. The disturbance compensator and the controller are both formulated in the discrete-time domain using the variable structure concept [19]. The actuator faults are estimated from the disturbance compensator and the control inputs are then modified (with the estimated fault signal) to achieve fault-tolerant control in the presence of pitch actuator faults. The proposed

Table 1. Gross Properties of the Wind Turbine [21].

Reference wind turbine	
Rated power	5MW
Number of blades	3
Rotor/Hub diameter	126m, 3m
Hub Height	90m
Cut-In, Rated, Cut-Out Wind Speed	3m/s, 11.4m/s, 25m/s
Rated generator speed (ω_{ng})	1173.7rpm
Gearbox ratio	97

techniques are validated using the aeroelastic wind turbine simulator software FAST [20]. This simulator is designed by the U.S. National Renewable Energy Laboratory's (NREL) National Wind Technology Center and widely used for studying wind turbine control systems. Since FAST is used by wind turbine researchers around the world, results based on this platform are more likely to be used by the wind industry than those based on a simpler model.

This paper is organized as follows. In Section 2, the onshore reference WT used in the simulations is introduced. In section 3 the baseline control strategy, that will be used for comparison, is recalled. In section 4 the control and disturbance estimation techniques are stated. The simulation results are presented in Section 5. Finally, Section 6 brings up the conclusions.

2. REFERENCE WT

Several FAST models of real and composite wind turbines of varying sizes are available in the public domain. In this work, the onshore version of a large WT that is representative of real utility-scale land- and sea-based multi-megawatt turbines described by [21] is used. This WT is a conventional three-bladed upwind variable-speed variable pitch controlled turbine. In fact, it is a fictitious 5MW machine with its properties based on a collection of existing wind turbines of similar rating since not all turbine properties are published by manufacturers. The main properties of this turbine are listed in Table 1. This work deals with the full load region of operation: that is, the proposed controller main objective is that the electric power follows the rated power.

Here, the generator-converter and the pitch actuators are modeled and implemented externally; i.e., apart from the embedded FAST code. The next subsections present these models as well as the wind model used in the simulations.

2.1 Wind modeling

In fluid dynamics, turbulence is a flow regime characterized by chaotic property changes. This includes low momentum diffusion, high momentum convection, and rapid variation of

pressure and velocity in space and time [22]. In the simulations, new wind data sets are generated in order to capture a more realistic turbulent wind simulation and, thus, to test the turbine controllers in a more realistic scenario. The turbulent-wind simulator TurbSim [23] developed by NREL is used. TurbSim generates a rectangular grid which holds the wind data. It can be seen from Fig. 1 that the wind speed covers the full load region as its values range from 12.91m/s up to the maximum of 22.57m/s.

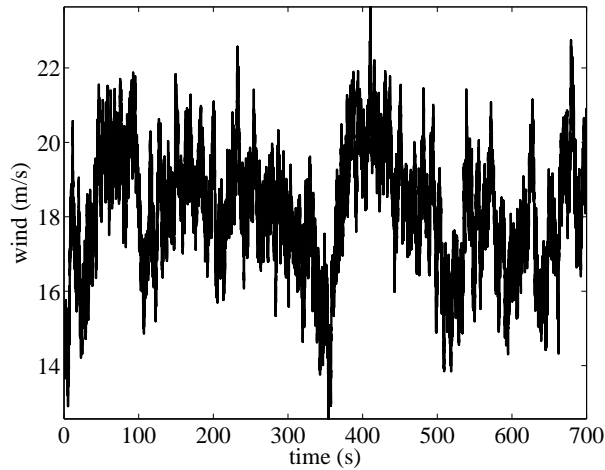


Figure 1. Hub-height wind speed for simulation tests. It is noteworthy the simulated wind gust from 350s to 400s (approximately) where wind speed moves from 12.91m/s up to the maximum of 22.57m/s and followed by an abrupt decrease in the next 100s.

2.2 Generator-converter actuator model

The dynamics of the generator-converter can be modeled by a first-order differential system [24], which is given by

$$\dot{\tau}_r(t) + \alpha_{gc}\tau_r(t) = \alpha_{gc}\tau_c(t),$$

where τ_r and τ_c are the real generator torque and its reference (given by the controller) respectively, where we set $\alpha_{gc} = 50$ [21]. And the power produced by the generator, $P_g(t)$, can be modeled using [24]

$$P_g(t) = \eta_g\omega_g(t)\tau_r(t),$$

where η_g is the efficiency of the generator and ω_g is the generator speed. In the numerical experiments $\eta_g = 0.98$ is used [24].

2.3 Pitch actuator model

The hydraulic pitch system consists of three identical pitch actuators, which are modeled as a linear differential equation with time-dependent variables, pitch angle $\beta(t)$ and its reference $u(t)$. In principle, it is a piston servo-system which can be expressed as a second-order

differential system [24]

$$\ddot{\beta}(t) + 2\xi\omega_n\dot{\beta}(t) + \omega_n^2\beta(t) = \omega_n^2u(t), \quad (1)$$

where ω_n and ξ are the natural frequency and the damping ratio respectively. For the fault-free case, the parameters $\xi = 0.6$ and $\omega_n = 11.11$ rad/s are utilized. [24].

2.4 Fault description

Faults in a WT have different degrees of severity and accommodation requirements. A safe and fast shutdown of the WT is necessary for some of them, while to others the system can be reconfigured to continue electrical power generation [25]. Variable structure controllers can be applied in the case of failures that gradually change system's dynamics [26]. In this work, pitch actuator faults are studied as they are the actuators with highest failure rate in WT [15]. A fault may change the dynamics of the pitch system by varying the damping ratio and natural frequencies from their nominal values to their faulty values in Equation 1. The parameters for the pitch system under different conditions are given in Table 2.

Table 2. Parameters for the hydraulic pitch system under different conditions [15].

Faults	ω_n (rad/s)	ξ
Fault-Free (FF)	11.11	0.6
High air content in oil (F1)	5.73	0.45
Pump wear (F2)	7.27	0.75
Hydraulic leakage (F3)	3.42	0.9

3. BASELINE CONTROL STRATEGY

The three-bladed 5MW reference WT given by FAST contains a torque and pitch controllers for the full load region, see [21]. In this section we recall these controllers and refer to them as the baseline torque and pitch controllers as their performance in the fault-free scenario will be used for comparison with the proposed FTC technique stated in Section 4.

The torque control and the pitch control, both, will use the generator speed measurement as input. To mitigate high-frequency excitation of the control systems, we filtered the generator speed measurement for both the torque and pitch controllers using a recursive, single-pole low-pass filter with exponential smoothing as proposed in [21].

In the full load region, the torque controller maintains constant the generator power, thus the generator torque is inversely proportional to the filtered generator speed, or,

$$\tau_c(t) = \frac{P_{\text{ref}}}{\hat{\omega}_g(t)}, \quad (2)$$

where P_{ref} is the reference power and $\hat{\omega}_g$ is the filtered generator speed. This controller will be referred as the baseline torque controller. As the generator may not be able to supply the desired

electromechanic torque depending on the operating conditions, and in the case of overshooting, the torque controller is saturated to a maximum of 47402.9Nm and a maximum rate limit of 15000Nm/s, see [21].

To assist the torque controller with regulating the WT electric power output, while avoiding significant loads and maintaining the rotor speed within acceptable limits, a collective pitch controller is added to the rotor speed tracking error. The collective blade pitch gain scheduling PI-controller (GSPI) is one of the first well-documented controllers and it is used in the literature as a baseline controller to compare the obtained results [15]. This work will follow the same steps and use the baseline GSPI controller to study the blade pitching system in the fault-free scenario. The GSPI is a collective pitch controller that employs a gain-scheduling technique to compensate for the nonlinearity in the turbine by changing the controller gain according to a scheduling parameter. This controller was originally developed by Jonkman for the standard land-based 5MW turbine [21]. The GSPI control has the generator speed as input and the pitch servo set-point, $\beta_r(t)$, as output. That is,

$$\beta_r(t) = K_p(\theta)(\hat{\omega}_g(t) - \omega_{ng}) + K_i(\theta) \int_0^t (\hat{\omega}_g(\tau) - \omega_{ng}) d\tau, \quad K_p > 0, K_i > 0, \quad (3)$$

where $\hat{\omega}_g(t)$ is the filtered generator speed, ω_{ng} is the nominal generator speed (at which the rated electrical power of the WT is obtained) and the scheduling parameter θ is taken to be the previous measured collective blade pitch angle. As the three pitch angles are measured, the collective pitch angle is obtained by averaging the measurements of all pitch angles. The scheduled gains are calculated following [21]. Finally, a pitch limit saturation to a maximum of 45° and a pitch rate saturation of $8^\circ/\text{s}$ is implemented, see [21].

4. FAULT TOLERANT CONTROL

This section details the design of the FTC strategy based on a control plus disturbance estimator in the time-discrete domain. The control objective is the tracking of the reference signal $\beta_r(t)$ (given by the baseline pitch controller, see Equation 3) and its corresponding velocity even in the case of pitch actuator fault. The block diagram in Figure 2 shows the connections between the WT (simulated using FAST), the FTC system, the pitch actuator and the torque and pitch controllers. To discretize continuous signals, a conventional sampler is used. As can be seen in the block diagram in Figure 2, a switch closes to admit an input signal every sampling period T_s . The sampler converts the continuous-time signal into a train of pulses occurring at the sampling instants kT_s for $k = 0, 1, 2, \dots$. Traditionally, a discrete-time signal is considered to be undefined at points in time between the sample times. In this work, discrete-time signals remain defined between sample times by holding on the value at the previous sample time. That is, when the value of a discrete signal is measured between sample times, the value of the signal at the previous sample time is observed. This is known as a *zero-order hold* or staircase generator as the output of a zero-order hold is a staircase function [27]. In this paper, the notation $[k]$ is used for these discrete-time signals.

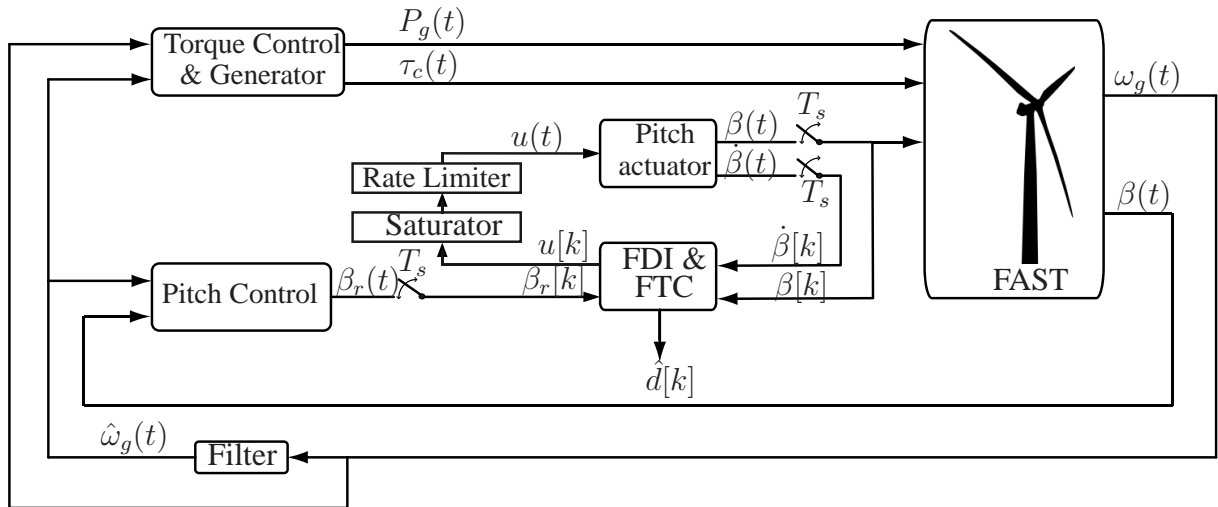


Figure 2. Block diagram of the closed loop system. Note that the torque control and the pitch control already include their respective saturator and rate limiter blocks.

Taking the pitch actuator system given in Equation 1, the state space representation in discrete-time, using Euler approximation¹, leads to

$$x[k+1] = (A + \Delta A)x[k] + bu[k] = Ax[k] + \Delta Ax[k] + bu[k] \quad (4)$$

where

$$x[k+1] = \begin{pmatrix} \beta[k+1] \\ \dot{\beta}[k+1] \end{pmatrix}, \quad A = \begin{pmatrix} 1 & T_s \\ -\omega_n^2 T_s & 1 - 2\xi\omega_n T_s \end{pmatrix}, \quad x[k] = \begin{pmatrix} \beta[k] \\ \dot{\beta}[k] \end{pmatrix}, \quad b = \begin{pmatrix} 0 \\ T_s\omega_n^2 \end{pmatrix} \quad (5)$$

where ΔA accounts for a fault in the system, and thus $\Delta Ax[k]$ is a disturbance term that will be estimated.

In order to design the control law $u[k]$, the control objective is that, even in a faulty case, the real pitch angle β follows the commanded reference pitch angle β_r (given by the pitch controller), as well as the velocity $\dot{\beta}$ follows the commanded reference $\dot{\beta}_r$. That is, the objective is to ensure the asymptotic convergence of the tracking error vector to zero. The error vector is defined as

$$e[k] = (e_1[k], e_2[k])^T = (\beta[k] - \beta_r[k], \dot{\beta}[k] - \dot{\beta}_r[k])^T.$$

Following the results in [19], the switching function is defined with the error vector and a column vector c as follows:

$$s[k] = c^T e[k], \quad (6)$$

¹For the ordinary differential equation $\dot{z} = f(z)$, the Euler discretization is defined as $\frac{z_{k+1} - z_k}{T_s} = f(z_k)$, such that $z_{k+1} = z_k + T_s f(z_k)$ where T_s is the sampling time [28].

and then, for system 5, the sliding surface 6 gives the asymptotic convergence of tracking error vector to zero designing vector c such that the matrix

$$\left[I - b (c^T b)^{-1} c^T \right] A \quad (7)$$

is contractive (eigenvalues inside the unit circle). When using a sample time $T_s = 0.0125$ (see [21]) and the fault-free values for the parameters ω_n and ξ , it is found that vector

$$c = (1, 0.25)^T$$

ensures that matrix 7 is contractive (with one eigenvalue equal to zero as in the application example given by [19]). Finally, to achieve the sliding mode, a new control law with a disturbance estimation law is proposed [19], as follows:

$$u[k] = -\hat{d}[k] + (c^T b)^{-1} \left[c^T \begin{pmatrix} \beta_r[k] \\ \dot{\beta}_r[k] \end{pmatrix} - c^T A x[k] + q s[k] - \eta \text{sgn}(s[k]) \right], \quad (8)$$

$$\hat{d}[k] = \hat{d}[k-1] + (c^T b)^{-1} g [s[k] - q s[k-1] + \eta \text{sgn}(s[k-1])], \quad (9)$$

where $0 \leq q \leq 1$, $0 < g < 1$, and $\eta > 0$ and being $\hat{d}[k]$ the fault estimator or also called the disturbance estimator. In the numerical simulations: $q = g = 1/2$ and $\eta = 100$. As can be seen in Equation 8, the proposed discrete controller for active FTC is dependent on a fault estimate, $\hat{d}[k]$, provided by the fault diagnosis system.

The pitch controller used by the FTC strategy is the baseline GSPI controller, see Section 3. On the other hand, the used torque controller is the chattering control proposed in [29], which is recalled here to be

$$\dot{\tau}_c(t) = \frac{-1}{\hat{\omega}_g(t)} \left[\tau_c(t)(a\hat{\omega}_g(t) + \dot{\hat{\omega}}_g(t)) - aP_{\text{ref}} + K_\alpha \text{sgn}(P_e(t) - P_{\text{ref}}) \right], \quad (10)$$

where P_{ref} is the reference power and P_e is the electrical power considered here (only for the control design) to be described as [30]

$$P_e(t) = \tau_c(t)\hat{\omega}_g(t), \quad (11)$$

where $\tau_c(t)$ is the torque control and $\hat{\omega}_g(t)$ is the filtered generator speed. This chattering controller, Equation 10, has several advantages (see [29]):

- Ensures that the closed-loop system has finite-time stability of the equilibrium point $(P_e(t) - P_{\text{ref}})$ and the settling-time can be chosen by properly defining the values of the parameters a and K_α .
- Does not require information from the turbine total external damping or the turbine total inertia. It only requires the filtered generator speed and reference power of the WT.

In the numerical simulations the values $a = 1$ and $K_\alpha = 1.5 \cdot 10^5$ have been used and a first order approximation of $\hat{\omega}_g(t)$ is computed.

This torque controller is saturated to a maximum of 47402.91Nm and a maximum generator torque rate saturation of 15000Nm/s, similarly to the baseline one.

5. SIMULATION RESULTS

The results compare the performance of the contributed FTC technique under different faulty scenarios with respect to the fault-free case with the baseline torque controller. When testing the FTC technique, the faults given in Table 2 are introduced only in the third pitch actuator (thus β_1 and β_2 are always fault-free) in the following way:

- From 0s to 100s, it is fault-free.
- From 100s to 200s, a fault due to high air content in oil (F1) is active.
- From 200s to 300s, it is fault-free.
- From 300s to 400s, a fault due to pump wear (F2) is active.
- From 400s to 500s, it is fault-free.
- From 500s to 600s, a fault due to hydraulic leakage (F3) is active.
- From 600s to 700s, it is fault-free.

The response of the generator velocity and electrical power are analyzed in terms of the normalized integral absolute error through the following performance indices:

$$J_w(t) = \frac{1}{t} \int_0^t |\omega_g(\tau) - \omega_{ng}| d\tau.$$

$$J_P(t) = \frac{1}{t} \int_0^t |P_g(\tau) - P_{ref}| d\tau.$$

As can be seen in Figure 3 (left) the three types of faults are detected by the disturbance estimator \hat{d} given in Equation 9. To finally setup the fault detection and isolation strategy, the proposed residual signal, $r(t)$, is computed as described in Figure 4 and its results shown in Figure 3 (right). This residual is close to zero when the system is fault-free. On the other hand, when a fault appears it is significantly affected and allows to isolate the type of fault (among the three studied pitch actuator faults stated in Table 2). The used thresholds to pinpoint the type of fault are:

- When the signal is smaller than 400 then F2 is detected. This can be seen in the zoom in Figure 3 (right)
- When the signal is between 400 and 5000 then F1 is detected.
- When the signal is above 5000 then F3 is detected.

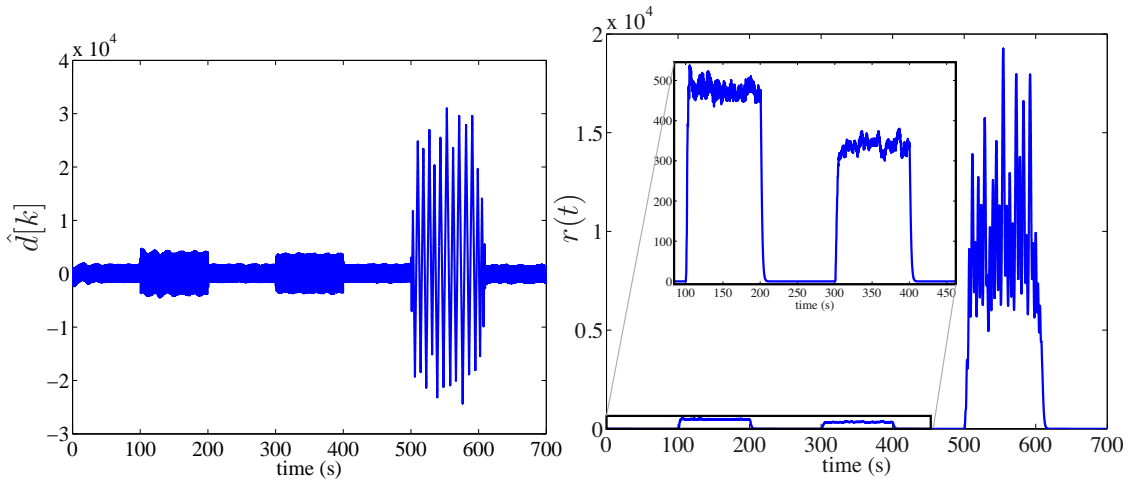
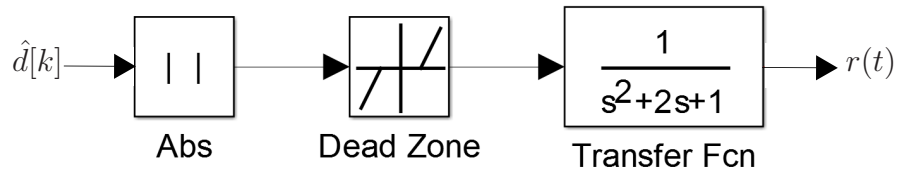


Figure 3. Disturbance estimator (left) and the residual signal (right).


 Figure 4. Computation of the continuous residual signal, $r(t)$. Note that the Simulink[®] dead zone block is used (start of dead zone value equal to 0 and end of dead zone value equal to 2000).

It can be seen from Figures 5 and 6 that the system behavior (electrical power and generator speed) with active fault compensation is similar to the behavior of the fault-free case, as the performance indices $J_P(t)$ and $J_w(t)$ values for the fault-free baseline and for the FTC (with faults) are very close. Moreover, the $J_w(t)$ performance index shows that the generator speed is closer to the nominal one during the faults F1 and F2 for the FTC than for the (fault-free) baseline controller. This can be seen in Figure 6 (right), as the values of the index, during the faults F1 and F2, are smaller for the FTC strategy.

Figure 7 (left) shows that the first pitch angle (β_1), which is always fault-free, has a slightly different behavior with the FTC than with the baseline control. This is due to the fact that with the FTC technique a fault is introduced in the third pitch actuator (β_3) as can be seen in Figure 7 (right). Although higher oscillations are present in the FTC, the pitch control signal is regulated within the authorized variation domain. That is, none of the variations exceed the mechanical limitations of the pitch actuator.

6. CONCLUSIONS

A WT fault-tolerant control scheme for pitch actuator faults is presented in this paper based on direct fault estimation by means of a disturbance compensator. With the proposed FTC

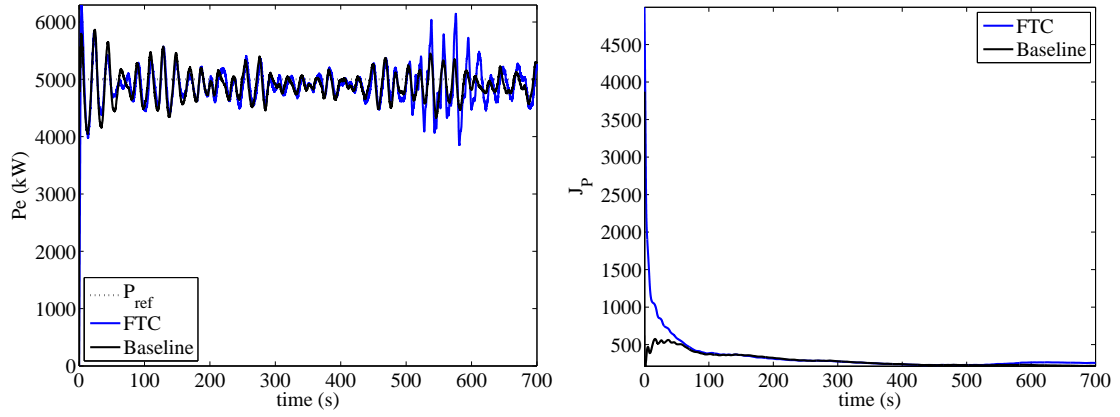


Figure 5. Electrical power (left) and J_p index (right).

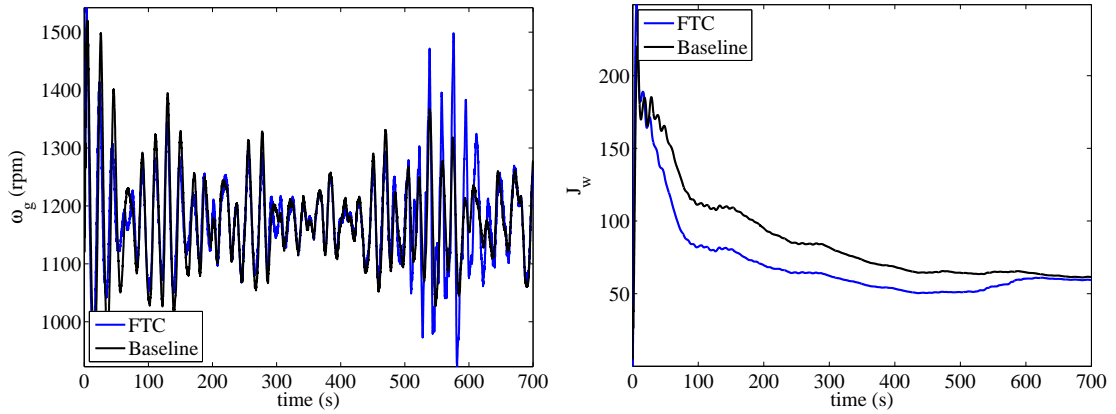


Figure 6. Generator speed (left) and J_w index (right).

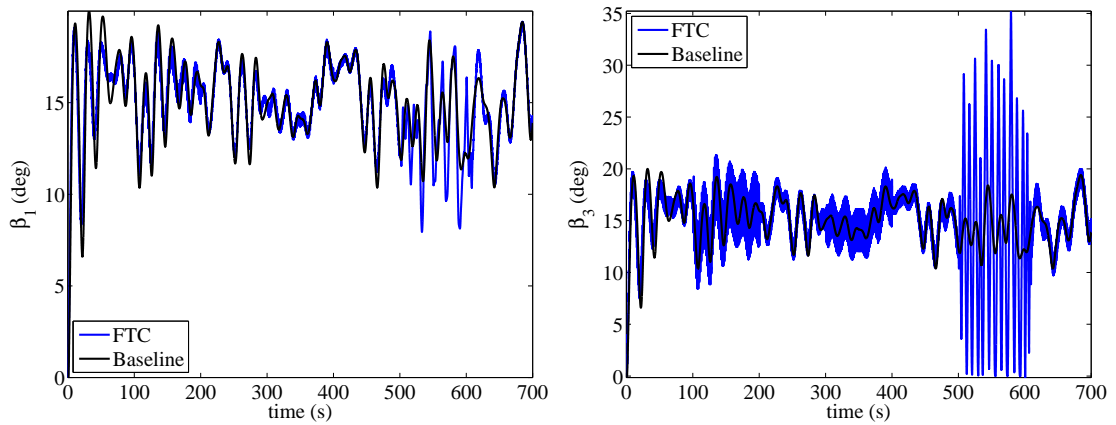


Figure 7. First pitch angle (left) and third pitch angle (right).

strategy, the system behavior in FAST simulations with faults is close to the behavior of the

baseline controllers in the fault-free case. Meanwhile, the proposed residual signal detects in short time the appearance of the faults. This is in itself a benefit for the development of fault diagnosis schemes for WT. Finally, note that the resulting FTC strategy can also be easily implemented in practice due to low data storage and simple math operations (at each sampling time, sums and products between scalars).

ACKNOWLEDGEMENTS

This work has been partially funded by the Spanish Ministry of Economy and Competitiveness through the research projects DPI2012-32375/FEDER and DPI2011-28033-C03-01, and by the Catalonia Government through the research project 2014 SGR 859.

References

- [1] Jianwu Zeng, Dingguo Lu, Yue Zhao, Zhe Zhang, Wei Qiao, and Xiang Gong. Wind turbine fault detection and isolation using support vector machine and a residual-based method. In *American Control Conference (ACC), 2013*, pages 3661–3666. IEEE, 2013.
- [2] Yolanda Vidal, Leonardo Acho, and Francesc Pozo. Robust fault detection in hysteretic base-isolation systems. *Mechanical Systems and Signal Processing*, 29:447–456, 2012.
- [3] Wei Chen, Steven X Ding, A Sari, Amol Naik, Abdul Qayyum Khan, and Shen Yin. Observer-based fdi schemes for wind turbine benchmark. In *Proceedings of IFAC World Congress*, pages 7073–7078, 2011.
- [4] Nassim Laouti, Nida Sheibat-Othman, and Sami Othman. Support vector machines for fault detection in wind turbines. In *Proceedings of IFAC World Congress*, volume 2, pages 7067–707, 2011.
- [5] Jianfei Dong and Michel Verhaegen. Data driven fault detection and isolation of a wind turbine benchmark. In *Proceedings of IFAC World Congress*, volume 2, pages 7086–7091, 2011.
- [6] Fariborz Kiasi, Jagadeesan Prakash, Sirish Shah, and Jong Min Lee. Fault detection and isolation of benchmark wind turbine using the likelihood ratio test. In *Proceedings of IFAC World Congress*, pages 7079–7085, 2011.
- [7] Jin Jiang and Xiang Yu. Fault-tolerant control systems: A comparative study between active and passive approaches. *Annual Reviews in control*, 36(1):60–72, 2012.
- [8] Pedro Casau, Paulo Andre Nobre Rosa, Seyed Mojtaba Tabatabaeipour, and Carlos Silvestre. Fault detection and isolation and fault tolerant control of wind turbines using set-valued observers. In *8th IFAC Symposium on Fault Detection, Supervision and Safety of Technical Processes*, pages 120–125, 2012.

- [9] Jiyeon Kim, Inseok Yang, and Dongik Lee. Control allocation based compensation for faulty blade actuator of wind turbine. In *Fault Detection, Supervision and Safety of Technical Processes*, volume 8, pages 355–360, 2012.
- [10] Damiano Rotondo, Fatiha Nejjari, Vicenc Puig, and Joaquim Blesa. Fault tolerant control of the wind turbine benchmark using virtual sensors/actuators. In *Fault Detection, Supervision and Safety of Technical Processes*, volume 8, pages 114–119, 2012.
- [11] S Simani and P Castaldi. Active actuator fault-tolerant control of a wind turbine benchmark model. *International Journal of Robust and Nonlinear Control*, 24(8-9):1283–1303, 2014.
- [12] Xiaoke Yang and Jan Maciejowski. Fault-tolerant model predictive control of a wind turbine benchmark. In *Proc. IFAC Safeprocess*, pages 337–342, 2012.
- [13] Lucy Y Pao and Kathryn E Johnson. Control of wind turbines. *Control Systems, IEEE*, 31(2):44–62, 2011.
- [14] Wenzhen Zhao, Lixue Qin, Xingjia Yao, and Guangkun Shan. Modeling research of mw wind turbine variable pitch system [j]. *Machine Tool & Hydraulics*, 6:056, 2006.
- [15] Rannam Chaaban, Daniel Ginsberg, and Claus-Peter Fritzen. Structural load analysis of floating wind turbines under blade pitch system faults. In Leonardo Acho Ningsu Luo, Yolanda Vidal, editor, *Wind Turbine Control and Monitoring*, pages 301–334. Springer, 2014.
- [16] Xiukun Wei, Michel Verhaegen, and Tim van Engelen. Sensor fault detection and isolation for wind turbines based on subspace identification and kalman filter techniques. *International Journal of Adaptive Control and Signal Processing*, 24(8):687–707, 2010.
- [17] Barry Dolan. *Wind Turbine Modelling, Control and Fault Detection*. PhD thesis, Technical University of Denmark, DTU, DK-2800 Kgs. Lyngby, Denmark, 2010.
- [18] Stijn Donders, V Verdult, and M Verhaegen. Fault detection and identification for wind turbine systems: a closed-loop analysis. *Master’s thesis, University of Twente*, 2002.
- [19] Yongsoon Eun, Jung-Ho Kim, Kwangsoo Kim, and Dong-II Cho. Discrete-time variable structure controller with a decoupled disturbance compensator and its application to a cnc servomechanism. *Control Systems Technology, IEEE Transactions on*, 7(4):414–423, 1999.
- [20] Jason Jonkman. NWTC computer-aided engineering tools (FAST), Last modified 28-October-2013.

- [21] J. M. Jonkman, S. Butterfield, W. Musial, and G. Scott. Definition of a 5-MW reference wind turbine for offshore system development. Technical report, National Renewable Energy Laboratory, Golden, Colorado, 2009. NREL/TP-500-38060.
- [22] Henk Kaarle Versteeg and Weeratunge Malalasekera. *An introduction to computational fluid dynamics: the finite volume method*. Pearson Education, 2007.
- [23] Neil Kelley and Bonnie Jonkman. NWTC computer-aided engineering tools (Turbsim), Last modified 30-May-2013.
- [24] PF Odgaard and KE Johnson. Wind turbine fault diagnosis and fault tolerant control - an enhanced benchmark challenge. In *Proc. of the 2013 American Control Conference–ACC,(Washington DC, USA)*, pages 1–6, 2013.
- [25] Fabiano Daher Adegas, Christoffer Sloth, and Jakob Stoustrup. Structured linear parameter varying control of wind turbines. In *Control of Linear Parameter Varying Systems with Applications*, pages 303–337. Springer, 2012.
- [26] Dohyeon Kim and Youdan Kim. Robust variable structure controller design for fault tolerant flight control. *Journal of Guidance, Control, and Dynamics*, 23(3):430–437, 2000.
- [27] Gene F Franklin, J David Powell, and Michael L Workman. *Digital control of dynamic systems*, volume 3. Addison-wesley Menlo Park, 1998.
- [28] Fernando Ornelas-Tellez, Edgar N Sanchez, and Alexander G Loukianov. Inverse optimal control for discrete-time nonlinear systems via passivation. *Optimal Control Applications and Methods*, 35(1):110–126, 2014.
- [29] Yolanda Vidal, Leonardo Acho, Ningsu Luo, Mauricio Zapateiro, and Francesc Pozo. Power Control Design for Variable-Speed Wind Turbines. *Energies*, 5(8):3033–3050, AUG 2012.
- [30] B. Boukhezzar, L. Lupu, H. Siguerdidjane, and M. Hand. Multivariable control strategy for variable speed, variable pitch wind turbines. *Renewable Energy*, 32(8):1273 – 1287, 2007.